Distinct Roles for Peroxisomal Targeting Signal Receptors Pex5 and Pex7 in *Drosophila*

Francesca Di Cara,[1,2] Richard A. Rachubinski, and Andrew J. Simmonds[2]
Faculty of Medicine and Dentistry, Department of Cell Biology, University of Alberta, Edmonton, Alberta T6G 2H7, Canada
ORCID IDs: 0000-0002-6973-3232 (F.D.C.); 0000-0001-9842-4327 (R.A.R.); 0000-0001-7165-9302 (A.J.S.)

ABSTRACT Peroxisomes are ubiquitous membrane-enclosed organelles involved in lipid processing and reactive oxygen detoxification. Mutations in human peroxisome biogenesis genes (*Peroxin*, *PEX*, or *Pex*) cause developmental disabilities and often early death. Pex5 and Pex7 are receptors that recognize different peroxisomal targeting signals called PTS1 and PTS2, respectively, and traffic proteins to the peroxisomal matrix. We characterized mutants of *Drosophila melanogaster Pex5* and *Pex7* and found that adult animals are affected in lipid processing. *Pex5* mutants exhibited severe developmental defects in the embryonic nervous system and muscle, similar to what is observed in humans with *PEX5* mutations, while *Pex7* fly mutants were weakly affected in brain development, suggesting different roles for fly Pex7 and human PEX7. Of note, although no PTS2-containing protein has been identified in *Drosophila*, Pex7 from *Drosophila* can function as a *bona fide* PTS2 receptor because it can rescue targeting of the PTS2-containing protein thiolase to peroxisomes in *PEX7* mutant human fibroblasts.

KEYWORDS peroxisome; peroxin; *Pex* gene; lipids; protein targeting; developmental defects

PEROXISOMES are involved in a variety of important biochemical functions, notably lipid metabolism and the detoxification of reactive species (De Duve and Baudhuin 1966; Bowers 1998; Wanders and Waterham 2006; Nguyen *et al.* 2008). Peroxisomes also have important roles in development, immune signaling, and viral maturation (Dixit *et al.* 2010; Smith and Aitchison 2013; You *et al.* 2015; Di Cara *et al.* 2017). Peroxisome biogenesis genes (*Peroxin*, *PEX*, or *Pex*) are, for the most part, conserved across the breadth of eukaryotes (Schrader and Fahimi 2006; Platta and Erdmann 2007). Thirteen *PEX* genes are required for peroxisome biogenesis in humans, and mutations in these genes cause the peroxisome biogenesis disorders, which manifest as heterogeneous syndromes with varied developmental defects (Braverman *et al.* 2013). PEX5 and PEX7 act as receptors that recognize signals, called peroxisome targeting signals (PTS), in soluble peroxisomal proteins to traffic them from the cytosol to the peroxisome matrix (Purdue *et al.* 1997; Klein *et al.* 2001; Ito *et al.* 2007; Smith and Aitchison 2013). PEX5 and PEX7 homologs are found across the eukaryota (McCollum *et al.* 1993; Rehling *et al.* 1996; Purdue *et al.* 1997; Kragler *et al.* 1998; Matsumura *et al.* 2000; Woodward and Bartel 2005; Lazarow 2006; Kanzawa *et al.* 2012). PEX5 recognizes the C-terminal PTS1 with the canonical sequence Ser-Lys-Leu (SKL), while PEX7 recognizes an N-terminal nonapeptide PTS2 with the consensus sequence (R/K)(L/V/I)X_5(H/Q)(L/A) (McCollum *et al.* 1993; Glover *et al.* 1994; Rehling *et al.* 1996; Shimozawa *et al.* 1999; Ito *et al.* 2007). Mutation of *PEX5* and *PEX7* gives rise to Zellweger spectrum disorder (ZSD) and rhizomelic chondrodysplasia punctata type 1 (RCDP1) (Purdue *et al.* 1997), respectively.

Patients with ZSD exhibit a spectrum of clinical phenotypes, with the most severely affected usually dying within their first year with profound neurologic impairment and liver failure. Patients with RCDP1 also exhibit a spectrum of clinical phenotypes, although generally of less severity than those seen in ZSD. Central nervous system (CNS) defects are prevalent in patients with RCDP1, including brains of decreased volume and deficient in both neurons and white matter, as well as progressive cerebellar degeneration. Defects in the β-oxidation of very-long-chain fatty acids (VLCFAs)

doi: https://doi.org/10.1534/genetics.118.301628
Manuscript received September 20, 2018; accepted for publication October 26, 2018; published Early Online November 1, 2018.
Supplemental material available at Figshare: https://doi.org/10.25386/genetics.7221503.
[1]Present address: Department of Microbiology and Immunology, Faculty of Medicine, Dalhousie University, Halifax, NS B3H 4R2, Canada.
[2]Corresponding authors: Faculty of Medicine and Dentistry, Department of Cell Biology, University of Alberta 5-14 Medical Sciences 8613 114 St. NW Edmonton, AB, Canada T6G 2H7. E-mail: dicara@dal.ca; andrew.simmonds@ualberta.ca

constitute a major pathology in patients with ZSD, while deficient plasmalogen (ether lipid) synthesis is a defining characteristic of patients with RCDP1 (Braverman *et al.* 2014).

Mutation of *Drosophila Pex* genes is linked to a range of phenotypes, including lethality (*Pex1*, *Pex3*, *Pex19*) and male sterility (*Pex16*) (Beard and Holtzman 1987; Chen *et al.* 2010; Mast *et al.* 2011; Nakayama *et al.* 2011; Faust *et al.* 2014; Bülow *et al.* 2018). In *Drosophila* Schneider 2 (S2) cells, knockdown of the *Pex5* transcript reduces targeting of PTS1-containing proteins to peroxisomes, while depletion or overexpression of the *Pex7* transcript leads to smaller or larger peroxisomes, respectively, than normal (Baron *et al.* 2016). However, the actual function of *Drosophila* Pex7 remains unclear, as no *bona fide* peroxisomal PTS2-containing protein has been identified in *Drosophila*; fly homologs of peroxisomal proteins use the PTS1/Pex5 pathway in *Drosophila*, *e.g.*, peroxisomal thiolase, trafficked by the PTS2/PEX7 import pathway in other organisms (Faust *et al.* 2012; Baron *et al.* 2016).

Here, we show that *Drosophila Pex5* mutants exhibit severe developmental defects in the embryonic nervous system and muscle, similar to that observed in patients with ZSD with *Pex5* mutations. *Pex7* fly mutants exhibited minor defects in brain development. We also show that *Drosophila* Pex7 can function as a *bona fide* PTS2 receptor because it can rescue targeting of the PTS2-containing protein thiolase to peroxisomes in *Pex7* mutant human fibroblasts.

Materials and Methods

Cell culture

Human fibroblasts were cultured in Dulbecco's modified Eagle's medium (ThermoFisher, Waltham, MA) supplemented with 10% fetal bovine serum, 50 units penicillin/ml, and 50 μg streptomycin sulfate/ml.

Fly husbandry, egg collection, and survival assays

Mutant lines $y^1 Mi\{y^{+mDint2} = MIC\} Pex5^{MI06050}\ w^*/FM7h$ (designated as $Pex5^{MI06050}$) and $y^1\ w^*$; $Mi\{y^{+mDint2} = MIC\}$ $Pex7^{MI14471}$ (designated as $Pex7^{MI14471}$); the Minos transposase strain $y^1\ w^*$; $sna^{Sco}/SM6a$, $P\{w^{+mC} = hsILMiT\}2.4$; the third chromosome deficiency line w^{1118}; *Df(3L)BSC816*, $P+PBac\{w^{+mC} = XP3.WH3\}BSC816/TM6C$, $Sb^1\ cu^1$ [designated *Df(3L)BSC816*]; and the X chromosome balancing line *FM7(GFP) Df(1)JA27/FM7c*, $P\{w^{+mC} = GAL4\text{-}Kr.C\}DC1$, $P\{w^{+mC} = UAS\text{-}GFP.S65T\}DC5$, sn^+ were from the Bloomington *Drosophila* Stock Center (BDSC). The y^1, w^* strain used as a control in all experiments and the *P{GAL4::VP16-nos.UTR}MVD2*, w^{1118} strain were from the BDSC. y^1, w^*; *UAS-dmPex7cDNA* was made by our laboratory. To make the $Pex5^{\Delta MI06050}$ strain, the MiMIC element was excised from the $Pex5^{MI06050}$ strain as verified by PCR (Venken *et al.* 2011). Flies were maintained at 25° on standard BDSC corn meal medium. $Pex5^{MI06050}$ mutants balanced over *FM7*(GFP) were allowed to lay eggs on apple juice agar plates for 2 days. On day 3, embryos were collected every 2 hr. GFP-negative embryos were incubated on apple juice agar plates at 25°. After 24 hr, hatched larvae were transferred to standard corn meal medium, and surviving animals were counted at the same time each day.

Geotaxis (climbing) assay

This assay was performed as described (Madabattula *et al.* 2015), using 20 flies (7 days old) per assay. Each assay had four technical replicates, and the assay was done 12 times for a total of 960 flies analyzed per genotype. Flies were transferred to a 250 ml glass graduated cylinder (ThermoFisher) sealed with wax film to prevent escape. Assays were conducted in ambient light at 22° and at the same time each day.

Lipid analysis

One thousand first-instar (L1) larvae (equivalent to 1 mg of protein extract) were homogenized in 1 ml of PBS buffer and sonicated for 5 min using a BioRuptor (Diagenode, Liège, Belgium) at low power. Lipids were extracted using chloroform: methanol (2:1) as described (Folch *et al.* 1957). Five micrograms of heptadecane (C_{17}) in chloroform was used as an internal control. Isolates were centrifuged at 3400 × *g*, and the chloroform phase containing lipids was passed through a sodium sulfate column (GE Healthcare Chicago, IL). The eluate was dried under nitrogen and resuspended in 100 μl of HPLC-grade hexane. Ten microliters of material were injected into an Agilent 6890 gas chromatograph with a flame-ionization detector. The amounts of VLCFAs were normalized to the relative amount of protein determined using a Qubit II fluorimeter (ThermoFisher). Nonesterified fatty acids (NEFAs) were analyzed as described (Bülow *et al.* 2018).

Quantitative RT-PCR analysis

Samples were rinsed twice with PBS, and total RNA was extracted using the RNeasy-Micro kit (QIAGEN, Valencia, CA). Next, 0.5–1 μg of RNA was reverse-transcribed using an iScript cDNA Synthesis kit (Bio-Rad, Hercules, CA). Quantitative RT-PCR (qRT-PCR) was performed (Realplex; Eppendorf, Hamburg, Germany) using KAPASYBR Green PCR master mix (Kapa Biosystems, Wilmington, MA). Samples were normalized to *RpL23* gene expression using the $2^{-\Delta\Delta CT}$ method (Livak and Schmittgen 2001). Sequences of qRT-PCR primers are as follows:

RpL23, 5′-GACAACACCGGAGCCAAGAACC, 5′-GTTTGCGCT GCCGAATAACCAC.
Pex5, 5′-AAATGCGAAGACATGGAACC, 5′-TGTAACGCACAC GGATGAAG.
Pex7, 5′-TCGAAATAGCCAGGCCATCAAG, 5′-AAGGAACCGA AGACAAGGACTC.

All qRT-PCR data are from three biological samples each tested in triplicate. Student's *t*-test was used to calculate the significance of differences in gene expression between averaged sample pairs.

Protein analysis and western blotting

Fifty microliters of cold Ephrussi–Beadle Ringer's solution supplemented with 10 mM EDTA, 10 mM DTT, 1× complete

protease inhibitor, and 1× PhosStop phosphatase inhibitor (Roche) were added to 3 × 10^6 pelleted cells. Twenty five microliters of 3× SDS-PAGE Buffer (Bio-Rad) containing 10 mM DTT at 70° were added to the homogenate and boiled for 10 min. Samples were resolved by SDS-PAGE on 10% acrylamide gels and transferred to nitrocellulose membranes (Bio-Rad). Membranes were blocked with 5% skim milk powder in TBS+Tween-20 (Tw) (150 mM NaCl, 20 mM Tris-HCl, pH 7.5, 0.05% Tween-20) for 1 hr and incubated for 16 hr with primary antibody in TBSTw. After washing three times for 5 min each with TBSTw, membranes were incubated with HRP-conjugated secondary antibody (Bio-Rad) at 1:10,000 dilution for 1 hr at 24°. Membranes were washed as above, and HRP activity was detected by enhanced chemiluminescence (Amersham, Piscataway, NJ). Primary antibodies were rabbit anti-active caspase 3 (BD Pharmingen) and mouse anti–α-tubulin (Sigma-Aldrich, St. Louis, MO).

Human PEX7 and Drosophila Pex7 complementary DNA cloning and transfection

The open-reading frame of human *PEX7* complementary DNA (cDNA; Braverman *et al.* 1997) was cloned into pENTR/D (ThermoFisher) using hPEX7-forward (5′-CACCATGAGTG CGGTGTGCGGTGG) and hPEX7-reverse (5′-GGTCAAGCA GGAATAGTAAGACAAG) primers. The *Drosophila Pex7* cDNA clone has been described (Baron *et al.* 2016). Both cDNAs were cloned into pT-Rex-DEST30 using LR Clonase (ThermoFisher). Clones were transiently transfected into immortalized human fibroblasts (Braverman *et al.* 1997) using the Amaxa Human Dermal Fibroblast Nucleofector kit (Lonza). Wild-type and *PEX7*^{null} fibroblasts were also mock-transfected using an empty DEST30 vector. *Drosophila Pex7* cDNA was inserted into pUASTattB and injected into the *y*^{1} *w*^{67c23}; *P{CaryP}attP40* strain to establish transgenic flies (BestGene).

Microscopy and image analysis

Human fibroblasts were fixed for 30 min in 4% paraformaldehyde in PBS, rinsed twice in PBST (PBS + 0.1% Triton X-100), and blocked for 1 hr in 5% normal goat serum (Sigma-Aldrich) before incubation for 16 hr at 4° with primary antibody. After four washes in PBST, cells were incubated with secondary antibody for 16 hr at 4°, washed four times in PBST, and mounted in Prolong-Gold (ThermoFisher). Images were captured using a C9100 camera (Hamamatsu) at 130 μm vertical spacing using a ×100 oil immersion objective (NA = 1.4) on a Zeiss AxioObserver M1 microscope coupled to an ERS spinning disk confocal microscope (PerkinElmer, Norwalk, CT). Primary antibodies were anti-mouse PMP70 (Sigma-Aldrich; Imanaka *et al.* 2000); anti-activated caspase 3 (BD Pharmagen), anti-phosphohistone H3 (Upstate Biotechnology), anti-SKL (Szilard *et al.* 1995), and anti-rat 3-ketoacyl-CoA thiolase (Bodnar and Rachubinski 1990). Secondary antibodies were Alexa Fluor 568 donkey anti-mouse, Alexa Fluor 488 donkey anti-rat, and Alexa Fluor 647 donkey anti-rabbit (Abcam, Cambridge, UK).

Embryos were maintained at 18°, collected every 16 hr, and processed for microscopy as reported (Parsons and Foley 2013). Antibodies to Futsch (22C10), raised by Seymour Benzer (California Institute of Technology), and to Even-skipped (2B8) and Repo (8D12), raised by Corey Goodman (University of California), were from the Developmental Studies Hybridoma Bank. Anti-myosin II was from Abcam (ab51098). All primary antibodies were diluted 1:20, and Alexa Fluor 568 donkey anti-mouse secondary antibody was diluted 1:1000. Terminal deoxynucleotidyl transferase dUTP nick end labeling (TUNEL) staining was performed as described (Parsons and Foley 2013). The volume of DAPI-stained brain volume was measured using Imaris three-dimensional analysis software (Bitplane) and optimized standard measurement protocols applied to all control and experimental samples for a particular data set. Third-instar larval length was measured using ImageJ. The number of anti-thiolase–labeled puncta was determined using ImageJ as described (Di Cara *et al.* 2017).

Measurement of NEFAs

NEFAs were measured using the copper-triethanolamine method. Tissue was homogenized in 20 μl chloroform + 1% Triton-X 100 per mg of tissue, and subjected to centrifugation at 13,000 × *g* for 10 min. The supernatant was removed and evaporated at 60°. Lipids were taken up in the same volume of phosphate buffer, and 25 μl of sample were transferred to a glass vial with 500 μl of chloroform/heptane (4:3). Vials were shaken for 2 min and subjected to centrifugation for 5 min at 2,000 × *g*. Three hundred microliters of the organic phase were transferred to a glass vial containing 250 μl of copper-triethanolamine, shaken for 2 min, and subjected to centrifugation for 5 min at 2,000 × *g*. One hundred fifty microliters of the organic phase were removed and evaporated at 60°. Lipids were taken up in 150 μl of ethanol, and vials were shaken for 15 min at 37°. Copper was detected by complexation with a mixture of dicarbazone–dicarbazide, and color intensity was measured in a 96-well plate at 550 nm in a microplate reader (TECAN, Männedorf, Switzerland).

Data availability

Strains and plasmids are available upon request. The authors state that all data necessary for confirming the conclusions presented are represented within the manuscript. Supplemental material available at Figshare: https://doi.org/10.25386/genetics.7221503.

Results and Discussion

Drosophila Pex5 is required for development

The *Pex5*^{MI06050} mutation resulted from a MiMIC insertion that disrupted the second exon of the coding region of *Pex5*-RA or the one exon of *Pex5*-RB (Venken *et al.* 2011). *Pex5* is on the X chromosome, and *Pex5*^{MI06050} mutants were lethal when homozygous or as hemizygous males with only 20% of embryos hatching (Figure 1, A–C). A further 15% of

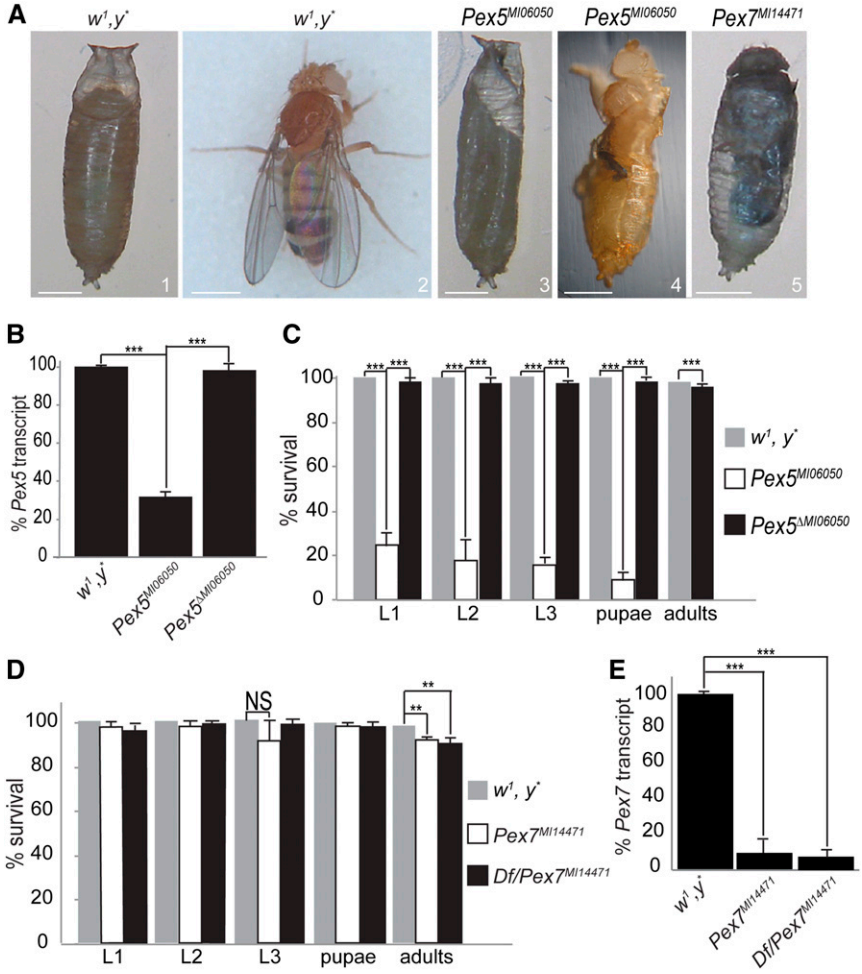

Figure 1 *Pex5* and *Pex7* mutants present developmental defects. (A) 1: Control (w^1, y^*) pupa 7 days after egg laying (AEL). 2: Control adults eclosed at day 9 AEL. 3: Most $Pex5^{MI06050}/Pex5^{MI06050}$ mutants arrested at the pseudo-pupal stage (day 11 AEL). 4: Some $Pex5^{MI06050}/Pex5^{MI06050}$ mutants die during eclosion (day 10 AEL). 5: Some $Pex7^{MI14471}/Pex7^{MI14471}$ mutants arrested at the pupa stage (day 11 AEL). Bar, 0.5 mm. (B) qRT-PCR measurement of *Pex5* messenger RNA levels in $Pex5^{MI06050}/Pex5^{MI06050}$ embryos and $Pex5^{\Delta MI06050}/Pex5^{\Delta MI06050}$ embryos, relative to control (w^1, y^*) embryos. Values are the averages of four independent experiments ± SD. (C) Most $Pex5^{MI06050}/Pex5^{MI06050}$ mutants die at the embryo stage, and none eclose as adults. $Pex5^{\Delta MI06050}/Pex5^{\Delta MI06050}$ mutants can eclose as adults like control flies. Values are the averages of four independent experiments ± SD 200 embryos were analyzed for each genotype. (D) Most $Pex7^{MI14471}/Pex7^{MI14471}$ mutants eclose as adults resembling the control (w^1, y^*) strain; however, ∼5% of $Pex7^{MI14471}/Pex7^{MI14471}$ embryos and $Df(3L)BSC816/Pex7^{MI14471}$ embryos arrest at the pupal stage. Values are the averages of four independent experiments ± SD; 200 embryos were analyzed for each genotype. (E) qRT-PCR confirms a reduction in *Pex7* transcript levels in $Pex7^{MI14471}/Pex7^{MI14471}$ and $Df(3L)BSC816/Pex7^{MI14471}$ ($Df/Pex7^{MI14471}$) embryos, relative to control (w^1, y^*) embryos. Values are the averages of four independent experiments ± SD. In B–E, significance was determined using Student's *t*-test; *** $P < 0.001$; ** $P < 0.01$; NS, not significant.

$Pex5^{MI06050}/Pex5^{MI06050}$ mutants died as larvae, with only 5% pupating (Figure 1, A and C, images 1–3). The 2% of pupae that survived died at eclosion (Figure 1, A and C, images 1–4). $Pex5^{MI06050}/Pex5^{MI06050}$ embryos had 35% of *Pex5* messenger RNA compared to controls (Figure 1B); maternally provided *Pex5* messenger RNA likely caused the phenotypic variability observed. Finally, the $Pex5^{\Delta MI06050}$ strain was viable and exhibited *Pex5* transcript levels comparable to those of the control w^1, y^* strain, supporting the hypothesis that the phenotypes observed in the mutant strains were due to *Pex5* disruption (Figure 1, B and C).

Mutations in human *PEX5* cause CNS, peripheral nervous system (PNS), and musculature defects (Steinberg *et al.* 2006; Braverman *et al.* 2013). We therefore evaluated CNS and PNS organization in $Pex5^{MI06050}$ mutant embryos compared to age-matched controls. In $Pex5^{MI06050}/Pex5^{MI06050}$ embryos, both the PNS and ventral nerve cord were disorganized (Figure 2A). Patients with peroxisome biogenesis disorders often show axonal demyelination (Braverman *et al.* 2013), and while *Drosophila* neurons are unmyelinated, wrapping glia play a role analogous to that of myelin (Freeman and Doherty 2006; Matzat *et al.* 2015). Glial cells were disorganized in $Pex5^{MI06050}/Pex5^{MI06050}$ embryos compared to controls (Figure 2A). Finally, the developing longitudinal and oblique musculature in late-stage $Pex5^{MI06050}/Pex5^{MI06050}$ embryos was also disorganized (Figure 2B).

Drosophila Pex5 is required for peroxisome biogenesis

We localized PTS1 (SKL)-containing proteins in third-instar larvae midgut cells to determine if the $Pex5^{MI06050}$ mutation affects PTS1-mediated peroxisome import. A punctate signal corresponding to peroxisomes with active PTS1 import was observed only in control w^1, y^* midgut cells, while an anti-SKL antibody cytosolic signal and anti-SKL–positive aggregates were observed in $Pex5^{MI06050}/Pex5^{MI06005}$ midgut cells, indicating compromised PTS1 import (Figure 2C). We profiled the spectrum of fatty acids in flies to examine the effects of $Pex5^{MI06050}$ mutation on systemic peroxisome function. $Pex5^{MI06050}/Pex5^{MI06050}$ embryos accumulated C_{22} and C_{24} VLCFAs and relatively lower levels of C_{14}, C_{16}, C_{18}, and C_{20} fatty acids compared to control embryos (Figure 2D). Increased apoptosis was seen in $Pex5^{MI06050}/Pex5^{MI06050}$ embryos as evidenced by their increased TUNEL staining compared to control embryos (Figure 2E).

Two transcript variants have been reported for *Drosophila Pex5* (http://flybase.org/reports/FBgn0023516). Humans have long and short transcripts for *PEX5*, with the long transcript encoding a PEX5 isoform that interacts with PEX7 and

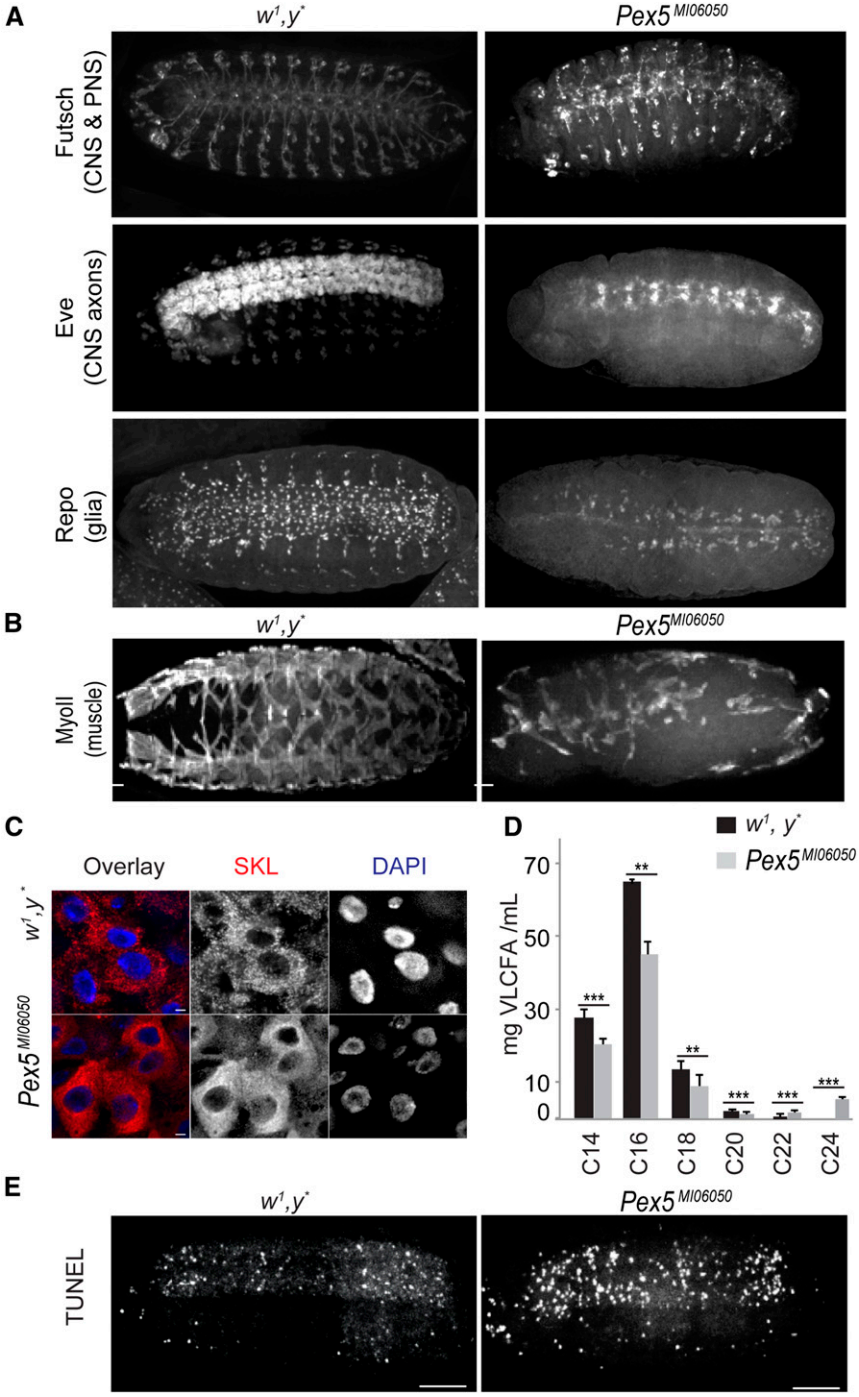

Figure 2 The *Pex5*^{MI06050} mutation affects CNS, PNS, and muscle structure. (A) The repeated segmental patterns of neurons of the CNS and PNS marked by anti-Futsch, CNS axons marked by anti-Even-skipped, and glial cells (except midline glia) marked by anti-Repo in control embryos (stage 15) were disrupted in *Pex5*^{MI06050}/*Pex5*^{MI06050} embryos. Bar, 10 μm. (B) The repeated segmental pattern of developing muscles marked by anti-myosin II (MyoII) in control embryos was disrupted in *Pex5*^{MI06050}/*Pex5*^{MI06050} embryos (stage 15). Bar, 10 μm. (C) Mature peroxisomes (punctate anti-SKL signal, red) are observed in the larval midgut. In *Pex5*^{MI06050}/*Pex5*^{MI060} mutants, diffuse cytosolic anti-SKL staining and anti-SKL–positive aggregates indicate PTS1 import was impaired. DAPI-labeled nuclei are in blue. Bar, 2 μm. (D) *Pex5*^{MI06050}/*Pex5*^{MI06050} mutants have lower amounts of C_{14}, C_{16}, C_{18}, and C_{20} fatty acids and greater amounts of C_{22} and C_{24} fatty acids compared to control animals. Values are averages of four independent experiments ± SD; 1000 larvae per sample per each genotype were used in each replicate (4000 larvae total). Significance was determined using Student's *t*-test; *** $P < 0.001$; ** $P < 0.01$. (E) *Pex5*^{MI06050}/*Pex5*^{MI06050} embryos exhibit greater numbers of TUNEL-positive cells than control embryos. Images are representative of five independent experiments. $N = 20$ per experiment per genotype. Bar, 10 μm.

functions as a chaperone in the import of PTS2-targeted proteins into the peroxisome (Otera *et al.* 2000). It would be interesting to characterize the roles of the Pex5 isoforms arising from the two *Pex5* transcripts in *Drosophila*, which does not have a PTS2 import pathway into peroxisomes (Faust *et al.* 2012; Baron *et al.* 2016).

Drosophila Pex7 is required for neuronal development

Pex7^{MI14471} arose by MiMIC insertion into the *Pex7* coding region (exon II) (Venken *et al.* 2011). Unlike *Pex5*^{MI06050}, *Pex7*^{MI14471}/*Pex7*^{MI14471} mutants were viable, with only 5% arresting at the pupal stage (Figures 1, A and D, images 1, 2, and 5). Similarly, animals carrying the *Pex7*^{MI14471} allele over a deletion covering the region *Df(3L)BSC816* (designated as *Df/Pex7*^{MI14471}) also showed ~5% arrest at the pupal stage (Figure 1D). Arrested pupae were the same size as control pupae but exhibited developmental abnormalities (Figure 1A, images 1, 2, and 5). qRT-PCR analysis showed *Pex7*^{MI14471}/*Pex7*^{MI14471} and *Df/Pex7*^{MI14471} embryos had ~10% of the levels of *Pex7* transcript relative to controls (Figure 1E). Because patients with RCDP1 exhibit defects in neurogenesis (Steinberg *et al.* 2006; Braverman *et al.*

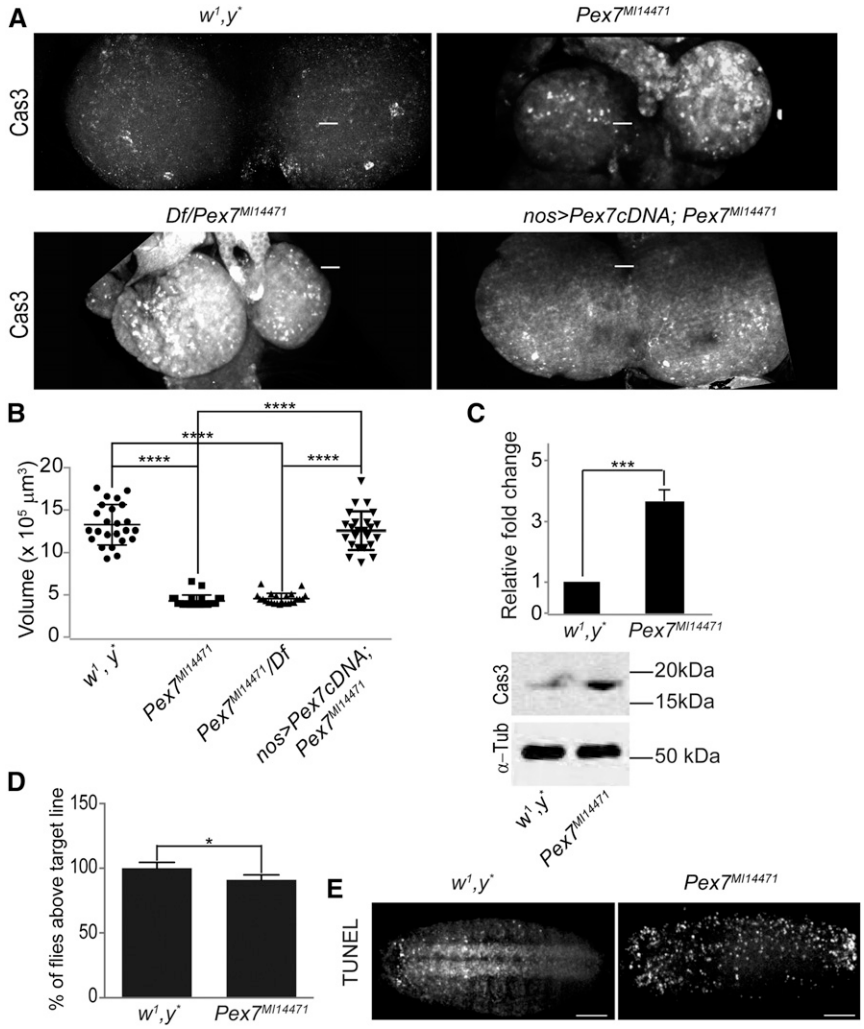

Figure 3 *Pex7* mutation causes defects in CNS development. (A) $Pex7^{MI14471}/Pex7^{MI14471}$ and $Df/Pex7^{MI14471}$ animals have smaller brains than animals of the control strain w^1, y^*. Overexpression of *Drosophila Pex7* cDNA using *nanos-GAL4* in $Df/Pex7^{MI14471}$ animals restores brain size to that of control animals. The number of apoptotic cells marked by activated caspase 3 (Cas3) was greater in brains of $Pex7^{MI14471}/Pex7^{MI14471}$ and $Df/Pex7^{MI14471}$ animals than in brains of control animals. Overexpression of *Drosophila Pex7* cDNA in $Df/Pex7^{MI14471}$ animals reduces the number of Cas3-positive cells in the brain to that observed in the brain of control animals. Bar, 10 μm (B) Loss of *Pex7* in $Pex7^{MI14471}/Pex7^{MI14471}$ and $Df/Pex7^{MI14471}$ animals results in reduced L3 brain volume compared to control L3 brain volume. Overexpression of *Drosophila Pex7* cDNA in $Df/Pex7^{MI14471}$ animals restores brain volume to that of brains of control animals. N = 15 per genotype. Significance was determined using one-way ANOVA; **** $P < 0.0001$. (C) Representative western blot and quantification showing activated Cas3 amounts are higher in $Pex7^{MI14471}/Pex7^{MI14471}$ L2-L3 brains than in control L2–L3 brains. α-Tubulin (α-Tub) served as a control for protein loading. Values represent the averages of four independent experiments ± SD. Significance was determined using Student's *t*-test; *** $P < 0.001$. (D) $Pex7^{MI14471}/Pex7^{MI14471}$ animals show reduced performance in a climbing assay that tests coordinated locomotion than do control animals. Values represent the averages of 12 independent experiments ± SD. N = 960 for each genotype. Significance was determined using Student's *t*-test; * $P < 0.05$. (E) $Pex7^{MI14471}/Pex7^{MI14471}$ embryos exhibit greater numbers of TUNEL-positive cells than control embryos. Images are representative of five independent experiments. N = 20 per experiment per genotype. Bar, 10 μm.

2013), we analyzed the brain morphology of $Pex7^{MI14471}/Pex7^{MI14471}$ third-instar larvae. Compared to the brains of control w^1, y^* larvae, the brains of $Pex7^{MI14471}/Pex7^{MI14471}$ larvae were smaller and of less volume (Figure 3, A and B). Although $Pex7^{MI14471}/Pex7^{MI14471}$ animals were slightly larger than control animals at the same stage (Supplemental Material, Figure S1, A and B), the mutation did not appear to affect developmental timing as most animals reached the adult stage at the same time as control animals. This observation is unusual in that small brain together with enlarged body size is usually associated with developmental arrest (Colombani *et al.* 2005; Mirth *et al.* 2005).

Reduced brain size could be due to either reduced cell proliferation or excess cell death (apoptosis) (Shklyar *et al.* 2014). The number of mitotic cells marked by the presence of phospho-Ser10-histone 3 (Wei *et al.* 1999) was similar in brains of control animals and $Pex7^{MI14471}/Pex7^{MI14471}$ animals (Figure S1C). Extracts of brain from $Pex7^{MI14471}/Pex7^{MI14471}$ animals had greater amounts of active caspase 3 compared to control extracts (Figure 3C). Also, there were more activated Caspase 3–positive cells in developing $Pex7^{MI14471}/Pex7^{MI14471}$ and $Df/Pex7^{MI14471}$ brains compared to control brain (Figure 3A). Overexpression of *Pex7* cDNA using the *nanos-Gal4* driver in $Pex7^{MI14471}/Pex7^{MI14471}$ animals rescued brain size and reduced activated caspase 3 staining to values observed in control animals (Figure 3, A and B), showing that these abnormal phenotypes exhibited by $Pex7^{MI14471}/Pex7^{MI14471}$ animals were due to dysfunctional *Pex7*. Increased apoptosis was observed in $Pex7^{MI14471}/Pex7^{MI14471}$ embryos as evidenced by their increased TUNEL staining compared to control embryos (Figure 3E), similar to $Pex5^{MI06050}/Pex5^{MI06050}$ embryos (Figure 2E).

We assayed neural and muscular function in flies by analyzing the ability of adults to exhibit a negative geotaxis response (Feany and Bender 2000; Madabattula *et al.* 2015). Control flies were more successful in the climbing assay than $Pex7^{MI14471}/Pex7^{MI14471}$ flies (Figures 3D and S1D).

Drosophila Pex7 has a role in peroxisome fatty acid processing

Lack of *Drosophila* PTS2 import calls into question if $Pex7^{MI14471}/Pex7^{MI14471}$-associated defects are linked to

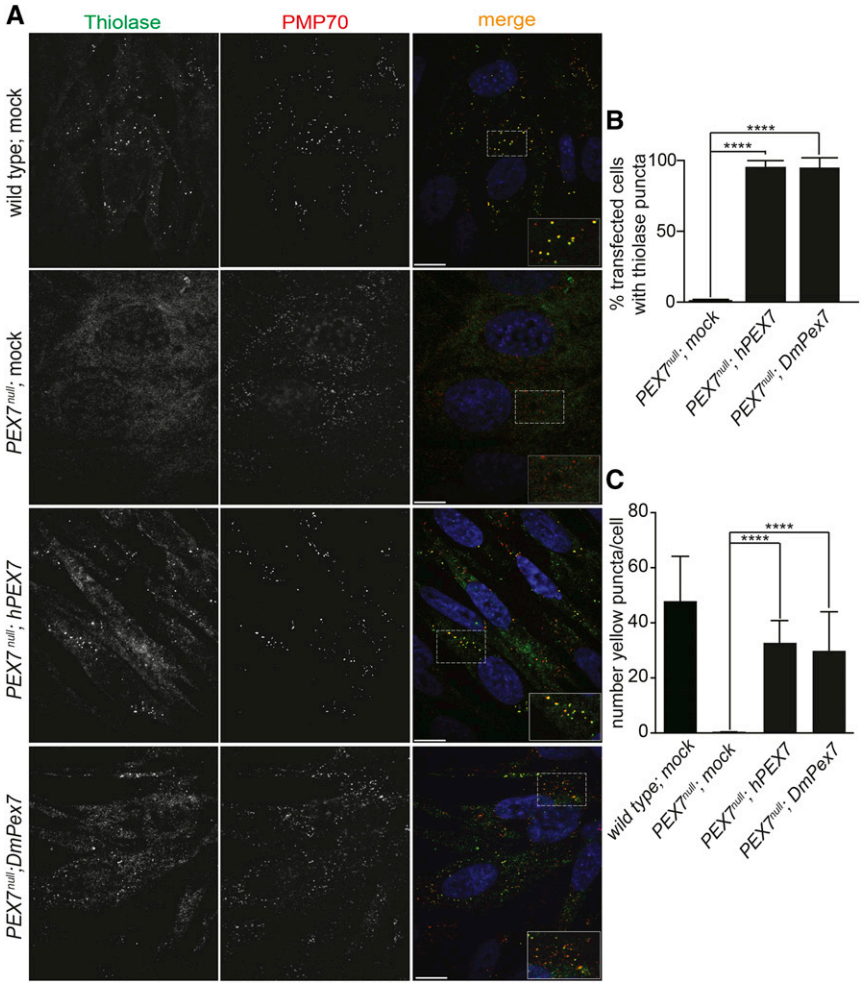

Figure 4 *Drosophila* Pex7 can restore PTS2 import in human cells. (A) In wild-type, mock-transfected human fibroblasts, anti-thiolase antibodies (Thiolase) decorate punctate structures characteristic of peroxisomes that also label with antibodies to the peroxisomal membrane protein PMP70. Mock-transfected *PEX7*^{null} fibroblasts do not exhibit punctate structures decorated by anti-thiolase antibodies, indicative of a failure to import thiolase into peroxisomes, but anti-PMP70 puncta remain, indicative of so-called "peroxisomal ghosts." Transfection of *PEX7*^{null} fibroblasts with human *PEX7* cDNA (*hPEX7*) restores thiolase import into peroxisomes. Transfection of *PEX7*^{null} fibroblasts with *Drosophila Pex7 cDNA* (*DmPex7*) also restores thiolase import into peroxisomes. Dashed boxes highlight regions expanded at the bottom right of the corresponding merged view. Bar, 10 μm. (B) Quantification of the percentage of cells exhibiting thiolase puncta in *PEX7*^{null}, *Pex7*^{null} transfected with *hPEX7*, and *Pex7*^{null} transfected with *DmPex7* fibroblasts. Values are the averages of four independent experiments ± SD. Each replicate used 20 cells per genotype (100 cells total). Significance was determined using one-way ANOVA; **** $P < 0.0001$. (C) Number of yellow puncta resulting from thiolase (green) and PMP70 (red) colocalization in wild-type, *PEX7*^{null}, *PEX7*^{null} transfected with *hPEX7*, and *PEX7*^{null} transfected with *DmPex7* fibroblasts. Values are the averages of four independent experiments ± SD. Each replicate used 20 cells per genotype (100 cells total). Significance was determined using one-way ANOVA; **** $P < 0.0001$.

peroxisome dysfunction. Circulating NEFAs are increased in amount in central obesity, insulin resistance, and diabetes and serve as a biomarker for these conditions (Boden 1998; Stich and Berlan 2004). Flies with dysfunctional peroxisomes have been shown to exhibit impaired lipid metabolism (Bülow *et al.* 2018; Di Cara *et al.* 2018). Similarly, we observed increased amounts of NEFAs in *Pex7*^{MI14471}/*Pex7*^{MI14471} larvae compared to control larvae (Figure S1E).

Drosophila Pex7 can functionally substitute for human PEX7 in PTS2 protein import

Human peroxisomal 3-ketoacyl-CoA thiolase, hereafter called thiolase, is imported into peroxisomes via the PTS2/PEX7 import pathway (Braverman *et al.* 1997). To determine if *Drosophila* Pex7 could function in PTS2 import into peroxisomes, we evaluated if expression of *Drosophila Pex7* cDNA (*DmPex7*) could reestablish thiolase import into peroxisomes in fibroblasts from a patient with RCDP1, which contain mutations in both copies of the *PEX7* gene (*PEX7*^{null}) (Braverman *et al.* 1997; Purdue *et al.* 1997). Transfection of the *PEX7*^{null} fibroblasts with a human *PEX7* cDNA (*hPEX7)* restored thiolase import into peroxisomes (Figure 4, A–C). Transfection of the *PEX7*^{null} fibroblasts with *DmPex7* cDNA also restored thiolase import into peroxisomes (Figure 4, A–C), indicating that *Drosophila* Pex7 is competent to mediate PTS2 import into peroxisomes.

The role of Drosophila Pex7 is divergent from the role of Pex7 proteins in other organisms

The localization of Pex7 to peroxisomes in *Drosophila* S2 cells (Baron *et al.* 2016), the changes in peroxisome size in S2 cells when *Pex7* transcript levels are reduced (Mast *et al.* 2011), and the altered lipid processing and changes in brain development we have now observed in *Pex7*^{MI14471}/*Pex7*^{MI14471} mutant flies clearly demonstrate a role for Pex7 in peroxisome biogenesis and/or function in *Drosophila*. However, the lack of a canonical PTS2 trafficking pathway in *Drosophila* calls into question how Pex7 functions in peroxisome biology in flies. *Drosophila* homologs of known yeast and human peroxisomal proteins with a PTS2 have instead a PTS1 (Faust *et al.* 2012; Baron *et al.* 2016). It is therefore likely that the canonical PTS2 import pathway into peroxisomes is not present in *Drosophila*, as evidenced by the failure of S2 cells to import a canonical PTS2-mCherry reporter into peroxisomes (Faust *et al.* 2012). Nevertheless, the extensive similarity in the primary structures of Pex7 proteins of *D. melanogaster*, *Saccharomyces cerevisiae*, *Arabidopsis thaliana*, *Danio rerio*, and *Homo sapiens* suggests conservation of

function of *Drosophila* Pex7 with Pex7 proteins from these other organisms (Figure S2). In contrast, the worm *Caenorhabditis elegans* does not have a PTS2 import pathway, but neither does it have a Pex7 homolog (Motley *et al.* 2000). It is possible that *Drosophila* has a divergent PTS2, but its identification and mechanism of recognition by Pex7 remain areas for future study.

Acknowledgments

We thank Nancy E. Braverman (McGill University) for advice and for providing wild-type and RCDP1 human fibroblasts; and the Lipidomics Core Facility at the University of Alberta, which is supported by funding from the Faculty of Medicine & Dentistry and the Women and Children's Health Research Institute, University of Alberta. This work was funded by a Collaborative Research Innovation Opportunities grant from Alberta Innovates – Health Solutions to R.A.R. and A.J.S., a Canadian Institutes of Health Research Foundation grant 143289 to R.A.R., and charitable support from The Edgar Foundation and the Ladies Auxiliary of the Fraternal Order of Eagles 3395 to R.A.R.

Literature Cited

Baron, M. N., C. M. Klinger, R. A. Rachubinski, and A. J. Simmonds, 2016 A systematic cell-based analysis of localization of predicted *Drosophila* peroxisomal proteins. Traffic 17: 536–553. https://doi.org/10.1111/tra.12384

Beard, M. E., and E. Holtzman, 1987 Peroxisomes in wild-type and rosy mutant *Drosophila melanogaster*. Proc. Natl. Acad. Sci. USA 84: 7433–7437. https://doi.org/10.1073/pnas.84.21.7433

Boden, G., 1998 Free fatty acids (FFA), a link between obesity and insulin resistance. Front. Biosci. 3: d169–d175. https://doi.org/10.2741/A272

Bodnar, A. G., and R. A. Rachubinski, 1990 Cloning and sequence determination of cDNA encoding a second rat liver peroxisomal 3-ketoacyl-CoA thiolase. Gene 91: 193–199. https://doi.org/10.1016/0378-1119(90)90088-9

Bowers, W. E., 1998 Christian de Duve and the discovery of lysosomes and peroxisomes. Trends Cell Biol. 8: 330–333. https://doi.org/10.1016/S0962-8924(98)01314-2

Braverman, N., G. Steel, C. Obie, A. Moser, H. Moser *et al.*, 1997 Human PEX7 encodes the peroxisomal PTS2 receptor and is responsible for rhizomelic chondrodysplasia punctata. Nat. Genet. 15: 369–376. https://doi.org/10.1038/ng0497-369

Braverman, N. E., M. D. D'Agostino, and G. E. Maclean, 2013 Peroxisome biogenesis disorders: biological, clinical and pathophysiological perspectives. Dev. Disabil. Res. Rev. 17: 187–196. https://doi.org/10.1002/ddrr.1113

Braverman, N. E., C. Argyriou, and A. Moser, 2014 Human disorders of peroxisome biogenesis: Zellweger spectrum and rhizomelic chondrodysplasia punctata, pp. 63–90 in *Molecular Machines Involved in Peroxisome Biogenesis and Maintenance*, edited by C. Brocard, and A. Hartig. Springer, Vienna. https://doi.org/10.1007/978-3-7091-1788-0_4

Bülow, M. H., C. Wingen, D. Senyilmaz, D. Gosejacob, M. Sociale *et al.*, 2018 Unbalanced lipolysis results in lipotoxicity and mitochondrial damage in peroxisome-deficient *Pex19* mutants. Mol. Biol. Cell 29: 396–407. https://doi.org/10.1091/mbc.E17-08-0535

Cara, F. D., M. H. Bülow, A. J. Simmonds, and R. A. Rachubinski, 2018 Dysfunctional peroxisomes compromise gut structure and host defense by increased cell death and Tor-dependent autophagy. Mol. Biol. Cell 29: 2766–2783. https://doi.org/10.1091/mbc.E18-07-0434

Chen, H., Z. Liu, and X. Huang, 2010 *Drosophila* models of peroxisomal biogenesis disorder: peroxins are required for spermatogenesis and very-long-chain fatty acid metabolism. Hum. Mol. Genet. 19: 494–505. https://doi.org/10.1093/hmg/ddp518

Colombani, J., L. Bianchini, S. Layalle, E. Pondeville, C. Dauphin-Villemant *et al.*, 2005 Antagonistic actions of ecdysone and insulins determine final size in *Drosophila*. Science 310: 667–670. https://doi.org/10.1126/science.1119432

De Duve, C., and P. Baudhuin, 1966 Peroxisomes (microbodies and related particles). Physiol. Rev. 46: 323–357. https://doi.org/10.1152/physrev.1966.46.2.323

Di Cara, F., A. Sheshachalam, N. E. Braverman, R. A. Rachubinski, and A. J. Simmonds, 2017 Peroxisome-mediated metabolism is required for immune response to microbial infection. Immunity 47: 93–106.e7 [corrigenda: Immunity 48: 832–833 (2018)]. https://doi.org/10.1016/j.immuni.2017.06.016

Dixit, E. S., Y. Boulant, A. S. Zhang, C. Lee, C. Odendall *et al.*, 2010 Peroxisomes are signaling platforms for antiviral innate immunity. Cell 141: 668–681. https://doi.org/10.1016/j.cell.2010.04.018

Faust, J. E., A. Verma, C. Peng, and J. A. McNew, 2012 An inventory of peroxisomal proteins and pathways in *Drosophila melanogaster*. Traffic 13: 1378–1392. https://doi.org/10.1111/j.1600-0854.2012.01393.x

Faust, J. E., A. Manisundaram, P. T. Ivanova, S. B. Milne, J. B. Summerville *et al.*, 2014 Peroxisomes are required for lipid metabolism and muscle function in *Drosophila melanogaster*. PLoS One 9: e100213. https://doi.org/10.1371/journal.pone.0100213

Feany, M. B., and W. W. Bender, 2000 A *Drosophila* model of Parkinson's disease. Nature 404: 394–398. https://doi.org/10.1038/35006074

Folch, J., M. Lees, and G. H. Sloane Stanley, 1957 A simple method for the isolation and purification of total lipides from animal tissues. J. Biol. Chem. 226: 497–509.

Freeman, M. R., and J. Doherty, 2006 Glial cell biology in *Drosophila* and vertebrates. Trends Neurosci. 29: 82–90. https://doi.org/10.1016/j.tins.2005.12.002

Glover, J. R., D. W. Andrews, S. Subramani, and R. A. Rachubinski, 1994 Mutagenesis of the amino targeting signal of *Saccharomyces cerevisiae* 3-ketoacyl-CoA thiolase reveals conserved amino acids required for import into peroxisomes *in vivo*. J. Biol. Chem. 268: 7558–7563.

Imanaka, T., K. Aihara, Y. Suzuki, S. Yokota, and T. Osumi, 2000 The 70-kDa peroxisomal membrane protein (PMP70), an ATP-binding cassette transporter. Cell Biochem. Biophys. 32: 131–138. https://doi.org/10.1385/CBB:32:1-3:131

Ito, T., S. Fujimura, Y. Matsufuji, T. Miyaji, T. Nakagawa *et al.*, 2007 Molecular characterization of the *PEX5* gene encoding peroxisomal targeting signal 1 receptor from the methylotrophic yeast *Pichia methanolica*. Yeast 24: 589–597. https://doi.org/10.1002/yea.1484

Kanzawa, N., N. Shimozawa, R. J. A. Wanders, K. Ikeda, Y. Murakami *et al.*, 2012 Defective lipid remodeling of GPI anchors in peroxisomal disorders, Zellweger syndrome, and rhizomelic chondrodysplasia punctata. J. Lipid Res. 53: 653–663. https://doi.org/10.1194/jlr.M021204

Klein, A. T., P. Barnett, G. Bottger, D. Konings, H. F. Tabak *et al.*, 2001 Recognition of peroxisomal targeting signal type 1 by the import receptor Pex5p. J. Biol. Chem. 276: 15034–15041. https://doi.org/10.1074/jbc.M010776200

Kragler, F., G. Lametschwandtner, J. Christmann, A. Hartig, and J. J. Harada, 1998 Identification and analysis of the plant peroxisomal targeting signal 1 receptor NtPEX5. Proc. Natl. Acad. Sci. USA 95: 13336–13341. https://doi.org/10.1073/pnas.95.22.13336

Lazarow, P. B., 2006 The import receptor Pex7p and the PTS2 targeting sequence. Biochim. Biophys. Acta 1763: 1599–1604. https://doi.org/10.1016/j.bbamcr.2006.08.011

Livak, K. J., and T. D. Schmittigen, 2001 Analysis of relative gene expression data using real-time quantitative PCR and the 2 (-Delta Delta C(T)) Method. Methods 25:402–408. https://doi.org/10.1006/meth.2001.1262

Madabattula, S. T., J. C. Strautman, A. M. Bysice, J. A. O'Sullivan, A. Androschuk *et al.*, 2015 Quantitative analysis of climbing defects in a Drosophila model of neurodegenerative disorders. J. Vis. Exp. (100): e52741. https://doi.org/10.3791/52741

Mast, F. D., J. Li, M. K. Virk, S. C. Hughes, A. J. Simmonds *et al.*, 2011 A *Drosophila* model for the Zellweger spectrum of peroxisome biogenesis disorders. Dis. Model. Mech. 4: 659–672. https://doi.org/10.1242/dmm.007419

Matsumura, T., H. Otera, and Y. Fujiki, 2000 Disruption of the interaction of the longer isoform of Pex5p, Pex5pL, with Pex7p abolishes peroxisome targeting signal type 2 protein import in mammals. Study with a novel Pex5-impaired Chinese hamster ovary cell mutant. J. Biol. Chem. 275: 21715–21721. https://doi.org/10.1074/jbc.M000721200

Matzat, T., F. Sieglitz, R. Kottmeier, F. Babatz, D. Engelen *et al.*, 2015 Axonal wrapping in the *Drosophila* PNS is controlled by glia-derived neuregulin homolog Vein. Development 142: 1336–1345. https://doi.org/10.1242/dev.116616

McCollum, D., E. Monosov, and S. Subramani, 1993 The *pas8* mutant of *Pichia pastoris* exhibits the peroxisomal protein import deficiencies of Zellweger syndrome cells–the PAS8 protein binds to the COOH-terminal tripeptide peroxisomal targeting signal, and is a member of the TPR protein family. J. Cell Biol. 121: 761–774. https://doi.org/10.1083/jcb.121.4.761

Mirth, C., J. W. Truman, and L. M. Riddiford, 2005 The role of the prothoracic gland in determining critical weight for metamorphosis in *Drosophila melanogaster*. Curr. Biol. 15: 1796–1807. https://doi.org/10.1016/j.cub.2005.09.017

Motley, A. M., E. H. Hettema, R. Ketting, R. Plasterk, and H. F. Tabak, 2000 *Caenorhabditis elegans* has a single pathway to target matrix proteins to peroxisomes. EMBO Rep. 1: 40–46. https://doi.org/10.1093/embo-reports/kvd010

Nakayama, M., H. Sato, T. Okuda, N. Fujisawa, N. Kono *et al.*, 2011 *Drosophila* carrying *Pex3* or *Pex16* mutations are models of Zellweger syndrome that reflect its symptoms associated with the absence of peroxisomes. PLoS One 6: e22984. https://doi.org/10.1371/journal.pone.0022984

Nguyen, S. D., M. Baes, and P. P. Van Veldhoven, 2008 Degradation of very long chain dicarboxylic polyunsaturated fatty acids in mouse hepatocytes, a peroxisomal process. Biochim. Biophys. Acta 1781: 400–405. https://doi.org/10.1016/j.bbalip.2008.06.004

Otera, H., T. Harano, M. Honsho, K. Ghaedi, S. Mukai *et al.*, 2000 The mammalian peroxin Pex5pL, the longer isoform of the mobile peroxisome targeting signal (PTS) type 1 transporter, translocates the Pex7p.PTS2 protein complex into peroxisomes via its initial docking site, Pex14p. J. Biol. Chem. 275: 21703–21714. https://doi.org/10.1074/jbc.M000720200

Parsons, B., and E. Foley, 2013 The *Drosophila* platelet-derived growth factor and vascular endothelial growth factor-receptor related (Pvr) protein ligands Pvf2 and Pvf3 control hemocyte viability and invasive migration. J. Biol. Chem. 288: 20173–20183. https://doi.org/10.1074/jbc.M113.483818

Platta, H. W., and R. Erdmann, 2007 Peroxisomal dynamics. Trends Cell Biol. 17: 474–484. https://doi.org/10.1016/j.tcb.2007.06.009

Purdue, P. E., J. W. Zhang, M. Skoneczny, and P. B. Lazarow, 1997 Rhizomelic chondrodysplasia punctata is caused by deficiency of human PEX7, a homologue of the yeast PTS2 receptor. Nat. Genet. 15: 381–384. https://doi.org/10.1038/ng0497-381

Rehling, P., M. Marzioch, F. Niesen, E. Wittke, M. Veenhuis *et al.*, 1996 The import receptor for the peroxisomal targeting signal 2 (PTS2) in *Saccharomyces cerevisiae* is encoded by the *PAS7* gene. EMBO J. 15: 2901–2913. https://doi.org/10.1002/j.1460-2075.1996.tb00653.x

Schrader, M., and H. D. Fahimi, 2006 Peroxisomes and oxidative stress. Biochim. Biophys. Acta 1763: 1755–1766. https://doi.org/10.1016/j.bbamcr.2006.09.006

Shimozawa, N., Z. Zhang, Y. Suzuki, A. Imamura, T. Tsukamoto *et al.*, 1999 Functional heterogeneity of C-terminal peroxisome targeting signal 1 in *PEX5*-defective patients. Biochem. Biophys. Res. Commun. 262: 504–508. https://doi.org/10.1006/bbrc.1999.1232

Shklyar, B., Y. Sellman, J. Shklover, K. Mishnaevski, F. Levy-Adam *et al.*, 2014 Developmental regulation of glial cell phagocytic function during *Drosophila* embryogenesis. Dev. Biol. 393: 255–269. https://doi.org/10.1016/j.ydbio.2014.07.005

Smith, J. J., and J. D. Aitchison, 2013 Peroxisomes take shape. Nat. Rev. Mol. Cell Biol. 14: 803–817. https://doi.org/10.1038/nrm3700

Steinberg, S. J., G. Dodt, G. V. Raymond, N. E. Braverman, A. B. Moser *et al.*, 2006 Peroxisome biogenesis disorders. Biochim. Biophys. Acta 1763: 1733–1748. https://doi.org/10.1016/j.bbamcr.2006.09.010

Stich, V., and M. Berlan, 2004 Physiological regulation of NEFA availability: lipolysis pathway. Proc. Nutr. Soc. 63: 369–374. https://doi.org/10.1079/PNS2004350

Szilard, R. K., V. I. Titorenko, M. Veenhuis, and R. A. Rachubinski, 1995 Pay32p of the yeast *Yarrowia lipolytica* is an intraperoxisomal component of the matrix protein translocation machinery. J. Cell Biol. 131: 1453–1469. https://doi.org/10.1083/jcb.131.6.1453

Venken, K. J., K. L. Schulze, N. A. Haelterman, H. Pan, Y. He *et al.*, 2011 MiMIC: a highly versatile transposon insertion resource for engineering *Drosophila melanogaster* genes. Nat. Methods 8: 737–743. https://doi.org/10.1038/nmeth.1662

Wanders, R. J., and H. R. Waterham, 2006 Biochemistry of mammalian peroxisomes revisited. Annu. Rev. Biochem. 75: 295–332. https://doi.org/10.1146/annurev.biochem.74.082803.133329

Wei, Y., L. Yu, J. Bowen, M. A. Gorovosky, and C. D. Allis, 1999 Phosphorylation of histone H3 is required for proper chromosome condensation and segregation. Cell 97: 99–109. https://doi.org/10.1016/S0092-8674(00)80718-7

Woodward, A. W., and B. Bartel, 2005 The *Arabidopsis* peroxisomal targeting signal type 2 receptor PEX7 is necessary for peroxisome function and dependent on PEX5. Mol. Biol. Cell 16: 573–583. https://doi.org/10.1091/mbc.e04-05-0422

You, J., S. Hou, N. Malik-Soni, Z. Xu, A. Kumar *et al.*, 2015 Flavivirus infection impairs peroxisome biogenesis and early anti-viral signaling. J. Virol. 89: 12349–12361. https://doi.org/10.1128/JVI.01365-15

Communicating editor: H. Bellen